JOURNAL OF MATERIALS SCIENCE 31 (1996) 765–771

Fracture mechanics behaviour of austenitic compacted graphite cast iron

CHENG-HSUN HSU, CHIH-KUANG HU, SHEN-CHIH LEE
Department of Materials Engineering, Tatung Institute of Technology, Taipei, Taiwan 10451

The fracture mechanics behaviour of high-nickel austenitic compacted graphite cast iron was studied and the effects of graphite morphology, alloying elements and specimen thickness on the mechanical properties, plane stress fracture toughness, and fatigue crack growth rate were evaluated. It was found that the graphite morphology, i.e. the percentage of compacted graphite present, was the major determinant of all properties of the materials investigated. The irons with a greater amount of compacted graphite (the balance was nodular graphite in austenitic matrix) resulted in lower tensile strength, yield strength, elongation and K_c fracture toughness but higher crack-growth index values (poorer crack-growth resistance). For 25 mm thick specimens, K_c values of the austenitic compacted graphite cast irons in this study were in the range of 58–64 MPa $m^{1/2}$. This is higher than ferritic/pearlitic ductile iron of 43–53 MPa $m^{1/2}$, and is compatible to Ni-resist austenitic ductile iron of 64.1 MPa $m^{1/2}$. The addition of cobalt not only contributed to slightly higher values of mechanical properties, but also higher plane stress fracture toughness and better crack growth resistance. Optical microscopy, scanning electron microscopy and X-ray diffraction techniques were applied to correlate the microstructural features to the properties attained.

1. Introduction

Nickel influences the structure of cast iron both as a graphitizer and austenite stabilizer [1]. Increasing the nickel content of cast iron leads to the formation of austenitic matrix. The nickel-base austenitic versions of grey and ductile cast iron have been well-established and are already enlisted as industrial standards [2–4]. They have been used in applications involving corrosion, wear resistance, high-temperature stability and strength [2, 5]. For the compacted graphite (CG) cast iron, the materials generally available are with ferritic and pearlitic matrices. However, there are limited research reports on the austenitic CG [6, 7] and virtually no available data on its fracture mechanics behaviour.

2. Experimental procedure

2.1. Casting processing

In reference to the basic chemical compositions of Ni-resist ductile iron [4], the austenitic compacted graphite irons were produced by using insufficient amounts of spheroidizer [2, 8, 9]. A 1 ton low-frequency induction furnace was used for melting the charge composed of 30% steel scrap, 45% returns and other alloying elements of nickel, chromium, manganese, and cobalt. Cobalt is known to improve thermal shock resistance and low thermal-expansion characteristics of austenitic grey iron [7]; in this study of austenitic CG iron, 5% cobalt was also added to determine its effects on mechanical properties. After melting down the elements, graphitizer and ferro-silicon were added to adjust the carbon-equivalent of the melt to the desired level. The melt was then superheated to 1540 °C (2804 °F) momentarily, and then tapped at 1500 °C (2732 °F) to the spheroidization treating ladle with Fe–Si as inoculant. Different amounts of spheroidizer, Ni–Mg alloy, were also added to the stream of the melt during tapping in order to obtain varying vermicularity (percentage of graphite in compacted/vermicular form) in the irons after solidification. The compositions of Fe–Si and Ni–Mg alloys are shown in Table 1. The treated iron was then poured at 1350–1450 °C (2462–2642 °F) to obtain Y-block castings (Fig. 1) in green sand moulds. Shake-out of the moulds was done 18 h after pouring. All the specimens were cut from the same-sized Y-block castings and machined to specific dimensions for various tests.

2.2. Chemistry and microstructural analysis

Chemical analysis of the as-cast materials was performed by using spectrometry and a carbon/sulphur analyser. Optical microscopy was applied at various magnifications to observe graphite morphology. It was determined by the aspect-ratio concept of Sofroni *et al.* [10] that at 1:1 ratio it is nodular graphite, between 1:2 and 1:10 it is compacted graphite, and beyond 1:11 it is flake graphite. In this paper, the definition of vermicularity is the amount of compacted graphite compared with nodular graphite.

0022–2461

TABLE I Chemical compositions of spheroidizer Ni–Mg and inoculant Fe–Si

	Composition (wt%)					
Additive	Si	Mg	Ca	Al	Ni	Fe
Ni–Mg	42	14–16	1.5–2.0	5.0–5.5	9–10	Bal
Fe–Si	70–75	–	–	–	–	Bal

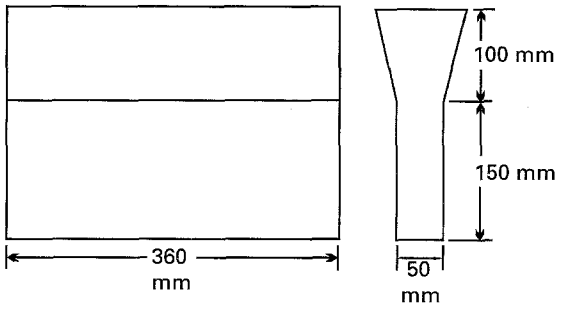

Figure 1 Dimensions of Y-block casting.

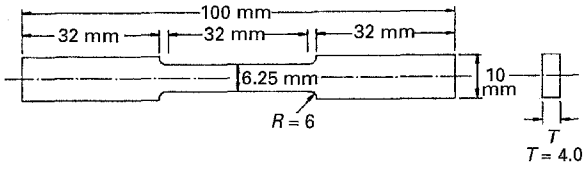

Figure 2 Dimensions of the specimen for tensile testing.

X-ray diffractometry was carried out for positive identification of the fully austenitic matrix [11].

2.3. Mechanical properties determination

A 25 ton capacity MTS hydro-servo dynamic testing machine was used for tensile, fracture toughness and fatigue crack growth testings. Dimensions of the tensile specimen were as shown in Fig. 2. Fracture toughness testing was performed in accordance to ASTM E-399 ([12] plane-strain) or ASTM E-561 ([13] plane-stress) with CT specimens 25, 10 and 5 mm thick. Fatigue crack rate experiments were conducted according to ASTM E-647 [14] with a specimen thickness of 5 mm. Hardness tests were carried out in Brinell hardness tester with a load of 500 kg. All mechanical testings were performed in an ambient environment.

3. Results and discussion

3.1. Chemical compositions and metallography

Chemical compositions of the test materials are listed in Table II. Table III illustrates the amount of spheroidizer/inoculant additions and the resulting microstructures. The materials shown in Figs 3 and 4 (with cobalt addition) were the austenitic irons produced in this study. No discernible difference, such as second phase particles, can be observed in these matrices with or without cobalt alloying. Thus, it may be assumed that cobalt has been completely dissolved in the matrix as solid-solution. The effect of the high nickel content on graphite morphology was that the free carbon seemed to be more in blocky form as compared with the standard unalloyed iron formation [1].

3.2. X-ray diffraction

The X-ray diffraction analysis confirmed that the as-cast structures produced were indeed fully austenite as expected. A typical diffraction pattern is shown in Fig. 5 whereby the five peaks were indexed to be γ-Fe (f c c) of the austenite.

TABLE II Chemical compositions of the resulting experimental cast irons

	Composition (wt%)									
Specimen	C	Si	Mn	P	S	Mg	Ni	Cr	Co	Fe
1	3.30	2.70	2.20	0.043	0.023	–	19.7	0.19	–	Bal
2	3.53	2.95	1.80	0.033	0.012	0.019	22.5	0.25	–	Bal
3	3.36	2.70	2.10	0.043	0.022	0.016	19.7	0.18	–	Bal
4	3.51	2.70	2.20	0.033	0.015	–	21.9	0.26	5.0[a]	Bal
5	3.71	2.75	1.80	0.031	0.012	0.019	22.7	0.24	5.0[a]	Bal
6	3.51	2.70	2.10	0.045	0.025	0.016	19.0	0.15	5.0[a]	Bal

[a]Amount of alloy addition to the melt.

TABLE III Amount of nodularizer and inoculant additions and the resulting as-cast microstructures of Y-block castings

Specimen	Spheroidizer (wt %)	Inoculant (wt %)	Matrix	Shape of graphite
1	–	0.3% Fe–Si	Austenite	Flake graphite (FG)
2	1.1% Ni–Mg	0.3% Fe–Si	Austenite	65%–75% Vermicularity (CG)
3	0.3% Ni–Mg	0.3% Fe–Si	Austenite	90%–95%Vermicularity (CG)
4	–	0.3% Fe–Si	Austenite	Flake graphite (FG)
5	1.1% Ni-Mg	0.3% Fe–Si	Austenite	65%–75% Vermicularity (CG)
6	0.3% Ni-Mg	0.3% Fe–Si	Austenite	90%–95% Vermicularity (CG)

[a] FG, grey iron; CG, compacted graphite iron. Vermicularity is the amount of free carbon in the form of compacted graphite, balance being nodular graphite.

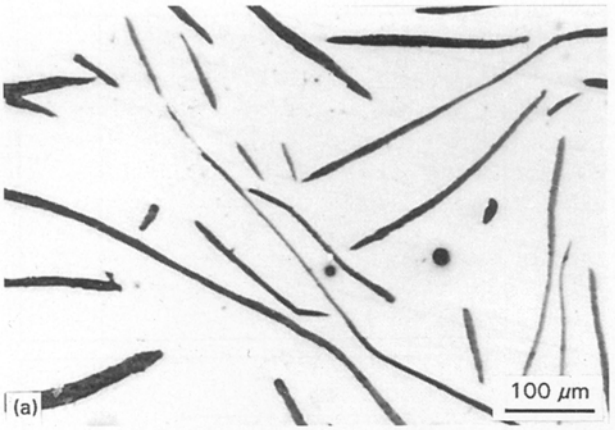

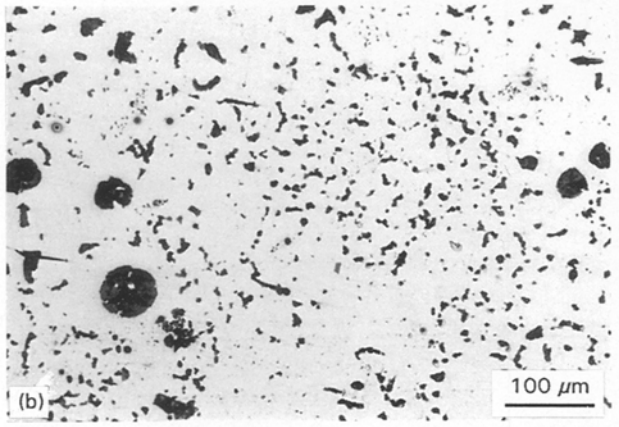

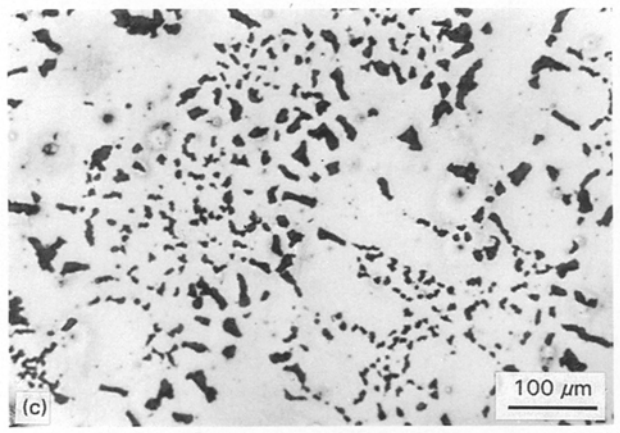

Figure 3 Microstructure of austenitic cast irons without cobalt addition: (a) specimen 1 flake graphite iron; (b) specimen 2 compacted graphite iron, 65%–75% vermicularity; (c) specimen 3 compacted graphite iron, 90%–95% vermicularity specimens; nital etched.

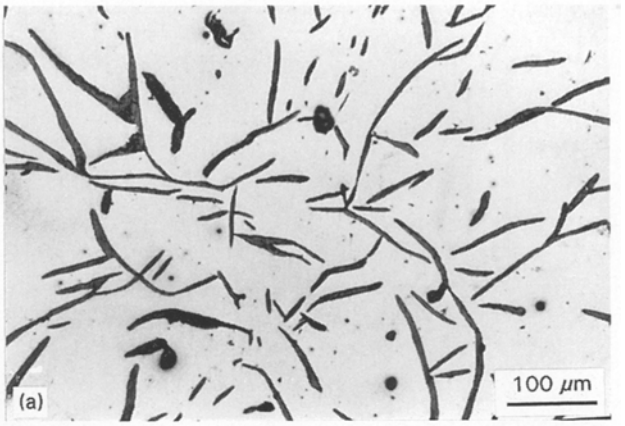

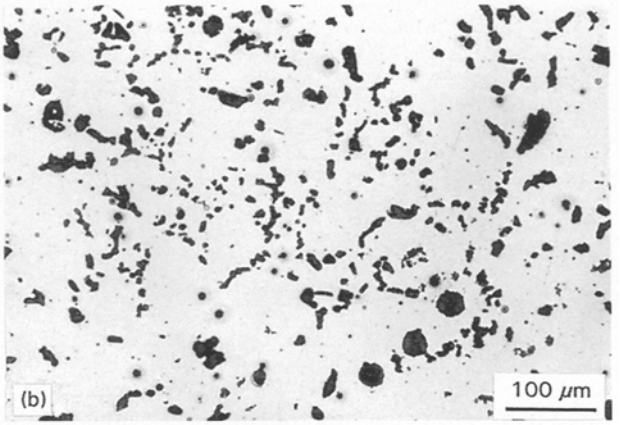

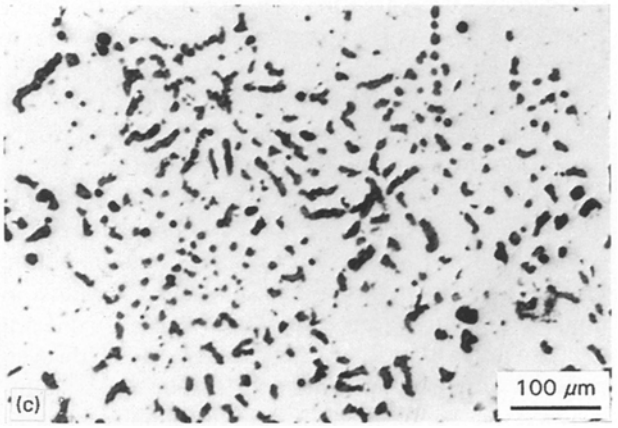

Figure 4 Microstructure of austenitic cast irons with cobalt addition: (a) specimen 1 flake graphite iron; (b) specimen 2 compacted graphite iron, 65%–75% vermicularity; (c) specimen 3 compacted graphite iron, 90%–95% vermicularity specimens; nital etched.

3.3. Mechanical properties

Table IV illustrates the mechanical properties of tensile and yield strengths, elongation, and Brinell hardness for austenitic matrix flake-graphite and compacted graphite cast irons. Fig. 6 illustrates the effects of vermicularity and the addition of cobalt on mechanical properties. Although the original purpose of the cobalt in cast iron was to improve the thermal-shock resistance and low thermal-expansion characteristics [7], due to solid-solution strengthening, the mechanical properties were also improved. The effect of graphite morphology was quite clear, in that compacted graphite iron exhibited strength properties (UTS = 247–325 MPa) superior to that of flake graphite irons (114–139 MPa) but inferior to ductile irons (379–449 MPa) [4]. Also, higher vermicularity (90%–95%) resulted in a reduction in strength. Although austenite is generally soft in nature, compacted graphite in the matrix limited the overall ductility from about 6.0%–20.0% elongation of the ductile irons [4] to that of 5.0%–10.9% for the CG irons in this study.

3.4. Fracture toughness

In this experiment, it was found that by using the compact tension (CT) specimens of 25 mm thickness,

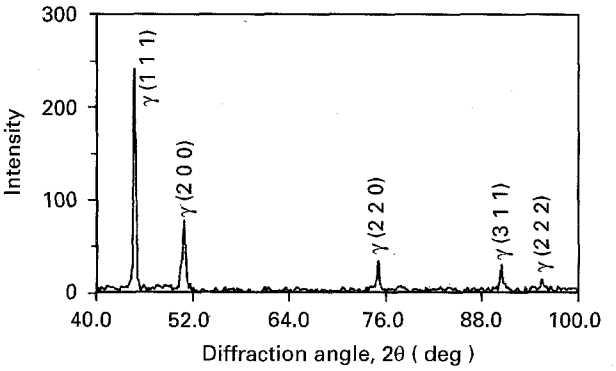

Figure 5 Typical X-ray diffraction pattern of austenitic cast irons (specimen 3)

TABLE IV Mechanical properties of austenitic FG and CG cast irons (all data are the average of three tests).

Specimen	UTS (MPa)	YS (MPa)	El (%)	Hardness (Brinell)
1(FG)	114	95	3.6	80
2(CG)	291	207	9.4	127
3(CG)	247	201	5.0	111
4(FG)	139	125	3.7	85
5(CG)	325	248	10.9	129
6(CG)	266	247	5.5	121

valid plane-strain fracture toughness K_{IC} values of the austenitic-matrix test materials could not be obtained. Thus, plane-stress fracture toughness K_C values were calculated in accordance to ASTM E-561 *R*-curve method. The specimens were 25, 10 and 5 mm thick, respectively. K_C data are listed in Table V. The 5% cobalt-doped materials (specimens 5 and 6) all exhibited K_C values higher than that of the non-cobalt materials (specimens 2 and 3). This was due primarily to the higher strength (via solid-solution strengthening of cobalt) such that the fracturing load in fracture toughness testing was higher and thus resulted in higher K_C values. Vermicularity (65%–90%), did not seem to alter the K_C values too greatly. However, material with a higher vermicularity did show a slightly lower K_C value, possibly for the same reasons as discussed above.

According to the concept of fracture toughness, particularly when the thickness of the specimen is reduced, the extent of plane strain diminishes while plane stress becomes more influential. Thus, it is necessary to study the effect of specimen thickness for actual applications of industrial designer fracture analysis. CT specimens of austenitic irons with thicknesses of 25, 10 and 5 mm were tested and the results are shown in Fig. 7. It can be seen from this figure that lesser the specimen thickness the higher is the K_C fracture toughness, as expected. Specimens that are 25 mm thick rendered toughness values of 58–64 MPa $m^{1/2}$, 10 mm thickness 75–86 MPa $m^{1/2}$, while a thickness of 5 mm gave 83–94 MPa $m^{1/2}$. Also listed in Table V, however, are the comparisons of the fracture toughnesses of CG and ductile irons using specimens [2] 25 mm thick. It can be seen that fracture toughness values of austenitic compacted graphite

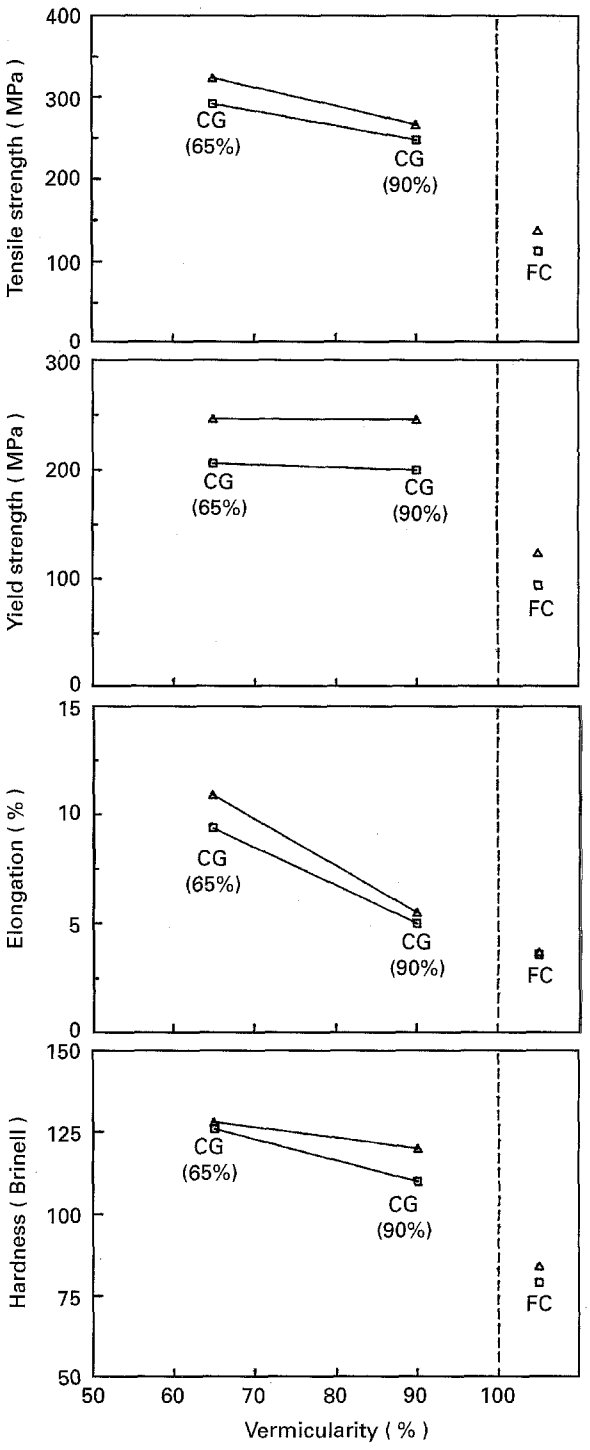

Figure 6 Effects of cobalt addition and vermicularity on mechanical properties of austenitic cast irons. (□) 20% Ni only, (Δ) 20% Ni and 5% Co; FC, grey iron; CG, compacted graphite iron.

irons (58–64 MPa $m^{1/2}$) were higher than those of ferritic/pearlitic ductile irons (43–52 MPa $m^{1/2}$) but compatible to Ni-resist ductile iron (64 MPa $m^{1/2}$).

In summary, although both the graphite morphology and the matrix structure were influential on fracture toughness, the matrix structure seemed to have a greater effect. In addition, the 5% cobalt-doped CG iron provided a K_C toughness value very close to austenitic ductile iron.

3.5. Fatigue crack growth rate

The results of the crack growth rate experiments are shown in Figs 8–11. Table V lists the *n* and *c* values

TABLE V Fracture toughness K_c values and crack growth rate parameter in the Paris equation of austenitic CG and ductile cast irons. (K_c data for specimens 1 and 4 austenitic grey iron were not obtained because CT specimens were fractured at loading-pin holes (13 mm diameter) during fatigue precracking in fracture toughness testing.)

Specimen	Fracture toughness (MPa $m^{1/2}$)			Parameter in Paris equation[a] (Specimen thickness 5 mm)	
	25 mm (K_c)	10 mm(K_c)	5 mm (K_c)	n	C
CG iron					
2(65–75% CG)	60.1	75.0	86.9	4.69	4.15×10^{-14}
3(90–95% CG)	58.2	71.3	83.3	5.34	6.19×10^{-15}
5(65–75% CG)	64.6	86.3	94.1	4.24	4.24×10^{-13}
6(90–95% CG)	62.3	82.4	91.3	4.66	7.55×10^{-14}
Ductile iron					
Ferritic	48.3				
Ferritic 1.55Si[b]	42.8				
Pearlitic D7003[b]	51.7				
Ni–resist D-5B[b]	64.1				

[a] Paris equation: $da/dN = C(\Delta K)^n$ where da/dN is crack growth rate, Δk is stress intensity variation, C and n are constants. Specifically, n is also called the crack growth rate index where lower n-values indicate better crack growth resistance.
[b] The fracture toughness values for ductile iron from [3].

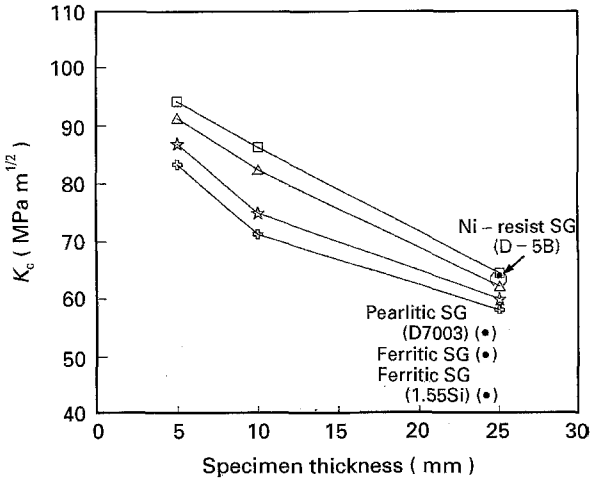

Figure 7 Effects of specimen thickness, (☆, □) 60 %–75%, (✠, Δ) 90%–95% vermicularity and cobalt addition on fracture toughness of austenitic CG cast irons. (●) Data for ductile iron (SG) [3] also plotted for comparison. (☆, ✠) 20% Ni, (□, Δ) 5% Co + 20% Ni.

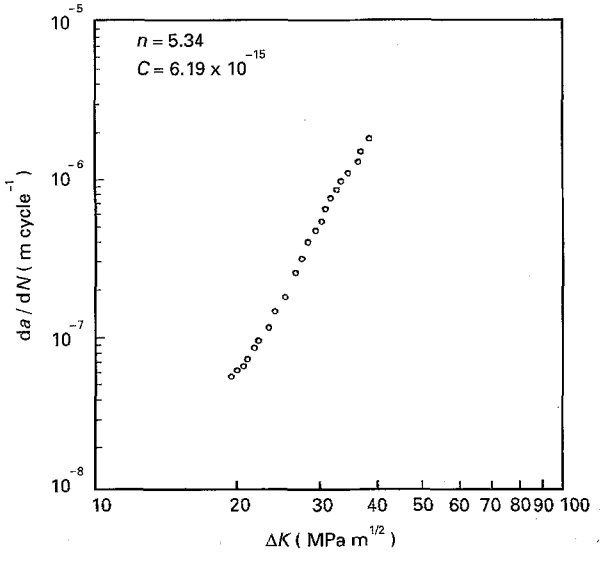

Figure 8 Fatigue crack growth test of specimen 2 compacted graphite iron, 65%–75% vermicularity, no cobalt.

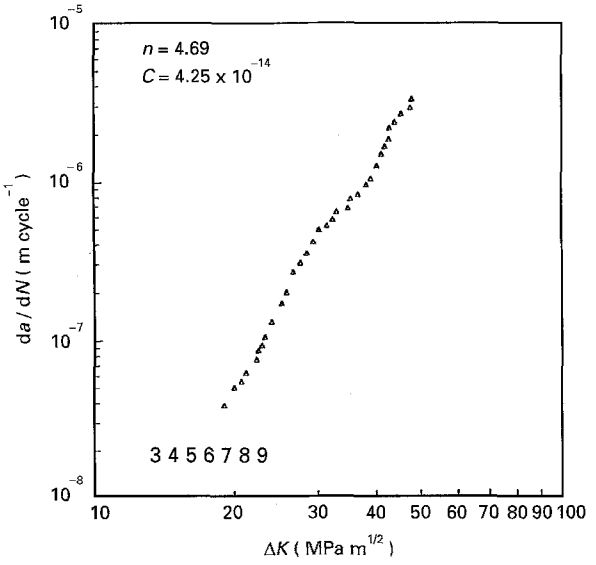

Figure 9 Fatigue crack growth test of specimen 3 compacted graphite iron, 90%–95% vermicularity, no cobalt.

derived from the Paris equation [15]. The significance of the n value was that a lower n value gave a better crack growth resistance [16] of the material. Materials with lower vermicularity and with cobalt addition rendered lower n-values. Also, there seemed to exist an inverse relationship between fracture toughness and crack growth resistance, i.e. the better the fracture toughness, the slower was the crack growth rate in fatigue. This is in agreement with what Knott [17] has proposed.

3.6. SEM fractography

Fractographic analysis was performed on the broken halves of the 25 mm thick CT specimens. Fig. 12a–c show the fracture appearance of the tested materials. Fig. 12a illustrates the typical brittle cleavage facets in grey iron with low fracture toughness. Fig. 12b and c show some ductile dimples and tearings of the

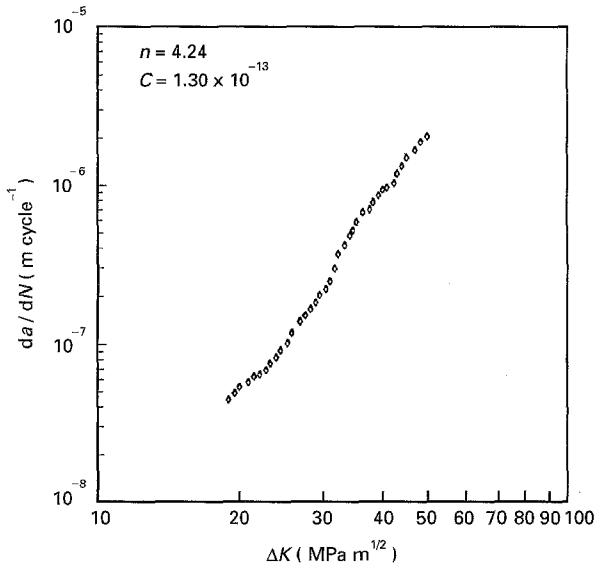

Figure 10 Fatigue crack growth test of specimen 5 compacted graphite iron, 65%–75% vermicularity, 5% cobalt added.

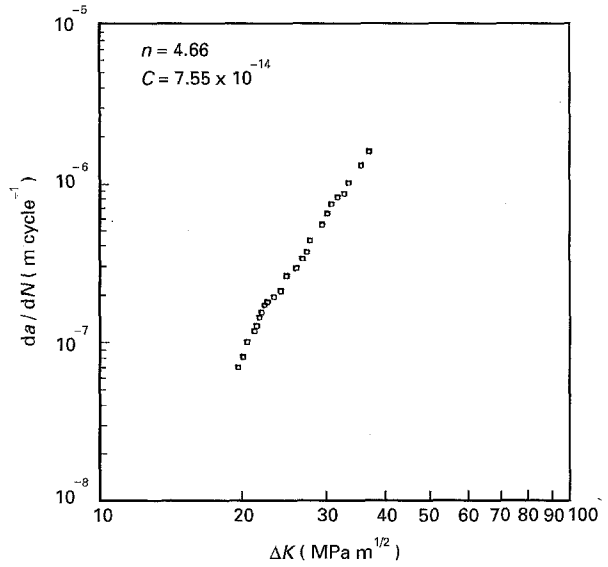

Figure 11 Fatigue crack growth test of specimen 6 compacted graphite iron, 90%–95% vermicularity, 5% cobalt added.

structure on a submicroscopical scale, indicating that fracturing of the CG irons was controlled to some extent by the matrix rather than the graphite morphology alone [16, 18]. In general, the more ductile fracture appearance present in the CG irons also explained the higher toughness values obtainable than that of the grey irons.

4. Conclusions

1. Addition of nickel at about 20% resulted in an austenitic matrix in all cast irons. Alloying with 5% cobalt improves both mechanical properties and fracture toughness, although not to a great extent.

2. Lower vermicularity (65%–70%) in austenitic compacted-graphite cast iron produced better properties than that of the high vermicularity (90%–95%).

3. Fracture toughness K_c values of austenitic compacted-graphite cast irons obtained in this study were

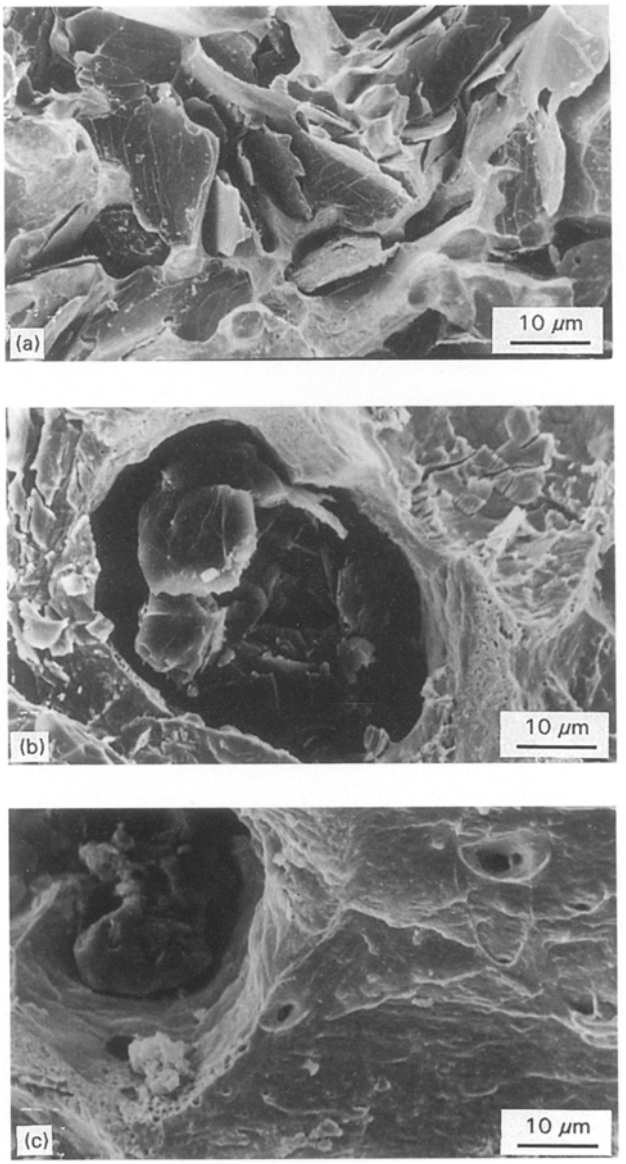

Figure 12 SEM fractography of austenitic cast iron: (a) specimen 1 flake graphite iron; (b) specimen 2 compacted graphite iron, 65%–75% vermicularity; (c) specimen 3 compacted graphite iron, 90%–95% vermicularity.

in the range of 58–94 MPa $m^{1/2}$ and it increased as the specimen thickness decreased.

4. Austenitic CG irons were found to possess higher fracture toughness characteristics than that of the ferritic and pearlitic ductile iron and compatible to Ni-resist austenitic ductile iron.

5. Crack growth rate da/dN values of the austenitic CG irons decreased as the corresponding fracture toughness increased.

Acknowledgement

The authors thank the National Science Council for Financial support under Contract NSC81-0405-E036-06.

References

1. I. MINKOFF, "The Physical Metallurgy of Cast Iron" (Wiley, New York, 1983) p. 185.
2. C. F. WALTON, in "Iron Castings Handbook" (Iron Casting Society, AFS, 1981) p. 231.

3. Annual Book of ASTM Standards, Vol. 1.02, A436, "Standard Specification for Austenitic Gray Iron Castings" (American Society for Testing and Materials, Philadelphia, PA, 1992) p. 229.
4. Annual Book of ASTM Standards, Vol. 1.02, A439, "Standard Specification for Austenitic Ductile Iron Castings" (American Society for Testing and Materials, Philadelphia, PA, 1992) p. 238.
5. R. B. GUNDLACH, in "ASM Metals Handbook" (American Society for Metals, Ohio, 1979) p. 699.
6. S. C. LEE and S. C. CHEN, *J. Chinese Mater. Sci.* **21** (1989) 210.
7. S. C. LEE and L. C. WONG, *Metall. Trans.* **22A** (1991) 1821.
8. W. H. LEE and S. C. LEE, *J. Tatung Inst. Tech. R.O.C.* **8** (1983) 59.
9. R. W. HERNE, C. R. LOPER Jr and P. C. ROSENTHAL, "Principles of Metal Casting" 2nd Edn (McGraw-Hill, Cleveland, 1967) p. 507.
10. L. SOFROMI, I. RIPOSAN and I. CHIRA, in "Proceedings of 2nd International Conference on Metallurgy of Cast Iron", (Georgi Publishing, Saphorim, Switzerland, 1975) p. 179.
11. B. D. CULLITY, "Elements of X-RAY Diffraction" (Addision-Wesley, London, 1978) p. 411.
12. Annual Book of ASTM Standards, Vol. 3.01, E399, "Plane-Strain Fracture Toughness of Metallic Materials" (American Society for Testing and Materials, Philadelphia, PA, 1992) p. 506.
13. Annual Book of ASTM Standards, Vol. 3.01, E561, "R-Curve Determination" (American Society for Testing and Materials, Philadelphia, PA, 1992) p. 597.
14. Annual Book of ASTM Standards, Vol. 3.01, E647, "Standard Test Method for Constant Load Amplitude Fatigue Crack Growth Rate" (American Society for Testing and Materials, Philadelphia, PA, 1992) p. 674.
15. P. C. PARIS and F. ERDOGAN, *Trans. ASME J. Basic Eng.* **85** (1963) 528.
16. A. F. HIBER, *AFS Trans.* **86** (1978) 143.
17. J. F. KNOTT, "Fundamentals of Fracture Mechanics" (Butterworths, London, Boston, 1973) p. 255.
18. S. C. LEE and C. C. LEE, *AFS Trans.* **88** (1989) 827.

Received 14 June 1994
and accepted 7 June 1995